Interactions between Adsorbed Hydrogenated Soy Phosphatidylcholine (HSPC) Vesicles at Physiologically High Pressures and Salt Concentrations

Ronit Goldberg,[†] Avi Schroeder,[‡§] Yechezkel Barenholz,[‡] and Jacob Klein[†*]

[†]Department of Materials and Interfaces, Weizmann Institute, Rehovot, Israel; [‡]Laboratory of Membrane and Liposome Research, Institute of Medical Research Israel-Canada, Hadassah Medical School, Hebrew University, Jerusalem, Israel; and [§]Department of Chemical Engineering, Ben Gurion University, Beer Sheva, Israel

ABSTRACT Using a surface force balance, we measured normal and shear interactions as a function of surface separation between layers of hydrogenated soy phosphatidylcholine (HSPC) small unilamellar vesicles (SUVs) adsorbed from dispersion at physiologically high salt concentrations (0.15 M $NaNO_3$). Cryo-scanning electron microscopy shows that each surface is coated by a close-packed HSPC-SUV layer with an overlayer of liposomes on top. A clear attractive interaction between the liposome layers is seen upon approach and separation, followed by a steric repulsion upon further compression. The shear forces reveal low friction coefficients (μ = 0.008–0.0006) up to contact pressures of at least 6 MPa, comparable to those observed in the major joints. The spread in μ-values may be qualitatively accounted for by different local liposome structure at different contact points, suggesting that the intrinsic friction of the HSPC-SUV layers at this salt concentration is closer to the lower limit (μ = ~0.0006). This low friction is attributed to the hydration lubrication mechanism arising from rubbing of the hydrated phosphocholine-headgroup layers exposed at the outer surface of each liposome, and provides support for the conjecture that phospholipids may play a significant role in biological lubrication.

INTRODUCTION

Phospholipid (PL) vesicles (liposomes) are often used in clinical applications, such as for drug delivery (1–4), and as biomembrane models (5), and their stability against aggregation or fusion has been extensively studied (6–11). Forces between model lipid bilayers have been measured directly in free dispersion as well as in supported bilayers (12–15). These forces have been described (12–15) in terms of double-layer electrostatic repulsion arising from surface charges, van der Waals attraction between the bilayers, and repulsion between the hydration layers that surround the lipid headgroups. Additional effects include repulsive steric effects arising from undulations (15) or from molecular protrusion (16) of individual headgroups from the layers, and attractive dipole-dipole interactions that may arise from correlated positioning of the opposing zwitterionic headgroups (12).

Microscopy studies of liposome or liposome assemblies on surfaces have been reported (17–19), and liposomes on surfaces have also been widely used as starting points for the creation of supported lipid bilayers formed by breaking-up and lateral spreading of the vesicles (20,21). To the best of our knowledge, however, no direct studies of interactions between liposomal surfaces, and particularly between surface-adsorbed liposome layers, have been reported to date. In a recent study (R. Goldberg, A. Schroeder, G. Silbert, K. Torgeman, Y. Barenholz, and J. Klein, unpublished), we used a surface force balance (SFB) to investigate the interactions between adsorbed layers of neutral (zwitterionic) PL liposomes, small unilamellar vesicles (SUVs) of hydrogenated soy phosphatidylcholine (HSPC) across water with no added salt. These liposomes formed a stable, uniform, close-packed array on the surfaces. As the surfaces approached, we observed a monotonically repulsive force between them, which we interpreted as being initially due to electrostatic double-layer effects and, upon closer approach, a steric component arising from the compressive distortion of the liposomes themselves. As the compressed liposome layers were made to slide past each other at increasing loads, an extremely low sliding friction coefficient μ, ($\mu \approx 10^{-4}$ – 10^{-5}) at mean pressures (P) up to >100 atmospheres (P > 10 MPa) was observed. We attributed this low friction to the hydration lubrication mechanism (arising as the highly hydrated phosphocholine groups exposed at the outer liposome surfaces slide past each other), as observed previously—generally at very much lower pressures—in a number of different systems (23–25).

In our previous study (R. Goldberg, A. Schroeder, G. Silbert, K. Torgeman, Y. Barenholz, and J. Klein, unpublished), we showed for the first time (to our knowledge) that phosphatidylcholine (PC) bilayers (comprising the liposome membrane) can provide physiological-level lubrication that is as efficient, or even more efficient, than that observed between articulating cartilage surfaces in hips or knees, at pressures (up to ~100 atm) that occur in major human joints.

Submitted November 3, 2010, and accepted for publication March 25, 2011.

*Correspondence: Jacob.klein@weizmann.ac.il

Avi Schroeder's present address is Department of Chemical Engineering and Koch Institute of Integrative Cancer Research, Massachusetts Institute of Technology, Cambridge, MA 02139.

Editor: Hagan Bayley.

0006-3495/11/05/2403/9 $2.00

doi: 10.1016/j.bpj.2011.03.061

This is of special interest because the molecular origin of the extremely efficient boundary lubrication in such joints is not well understood (26,27). Indeed, it is the topic of a long-standing controversy between those who hold that it arises from macromolecules (such as lubricin (28), hyaluronic acid (29), or aggrecans (30)) at the cartilage-synovium interface, and those who conjecture that is due to surface-active PL layers coating the rubbing surfaces in a boundary lubrication mode (26) somewhat like that found in classical engineering tribology (i.e., where the alkyl tails of the surfactant layers rub past each other (31)). In the investigation presented here, we extend our earlier study, which was carried out in pure water (i.e., with no added salt), to the case of concentrated salt solutions, to better examine the relevance of our results under biological ion concentrations. The main experimental approach we used to directly measure both normal and frictional interactions between the HSPC-SUVs-coated surfaces is based on the SFB. In addition, we used high-resolution cryo-scanning electron microscopy (cryo-SEM) to image the surface structures directly.

MATERIALS AND METHODS

Full details are provided in the Supporting Material.

Liposomes preparation

We synthesized SUVs of HSPC (molecular mass = 762.10 g/mol, >99% purity; Lipoid, Ludwigshafen, Germany) using standard approaches (32) by progressive downsizing from multilamellar vesicles prepared by hydrating the lipids in 150 mM $NaNO_3$ at 62°C (above the gel-to-liquid crystalline phase transition temperature, T_m, of HSPC, 53°C (32); for a schematic of the molecule, see Fig. 2, *inset*). The nitrate group was chosen as the counterion because of its compatibility with our experimental system (the mica surfaces in the SFB are back-silvered, and this coating was found to be sensitive to some ions (notably Cl^-), which cause degradation of the silver layer).

Dynamic light scattering

Liposomes were characterized for size distribution by dynamic light scattering (DLS). The DLS data indicated that >95% of the liposomes in the bulk solution were 75 ± 3 nm in diameter.

Measurement of the ζ potential

HSPC-SUVs in low (5 mM) salt concentrations had a ζ potential of 6.20 ± 0.26 mV, whereas at the high salt concentrations used in our study (0.15 M), the ζ-potential values, measured with somewhat lower accuracy, were in the range of 1.3 ± 0.6 mV, demonstrating the neutral nature of the zwitterionic lipids.

Determination of PL concentration

We determined the PL concentrations by using the modified Bartlett assay as described elsewhere (33).

Surface preparation

We adsorbed the HSPC-SUVs on an atomically smooth mica surface by placing freshly cleaved mica in 10 ml 150 mM $NaNO_3$ and then adding 360 ± 10 μL of the SUV dispersion (of 30 mM HSPC PL concentration) for 1.5–2 h of incubation at room temperature. We then washed the mica surfaces to remove excess, nonadsorbed liposomes by placing the adsorbed surfaces in a beaker filled with 150 mM $NaNO_3$ for few minutes along with a delicate shaking motion. All preparations were done in a laminar flow hood to prevent contamination.

Cryo-SEM

Cryo-SEM samples (mica surfaces covered with HSPC liposomes) were prepared as described above. Water was sublimed at −80°C for 2 h, and samples were rotary-shadowed with 3 nm Pt at an angle of 45°.

SFB

We measured the normal and lateral force profiles using the SFB between the two atomically smooth mica surfaces, as described in detail elsewhere (34) and in the Supporting Material (also see Fig. 2, *inset*). The surfaces were incubated for 1.5–2 h in liposome dispersion to enable adsorption of the HSPC-SUVs to take place, and then rinsed and remounted in the SFB. The results shown are from three different experiments and different contact points within each experiment (approximately nine in all).

RESULTS

Cryo-SEM images

Fig. 1 shows cryo-SEM micrographs of HSPC liposomes adsorbed from a 150 mM $NaNO_3$ solution onto mica and adhering densely to the surface. The liposome coating is composed of a close-packed layer of liposomes in contact with the substrate, with a sparser irregular coating of excess liposomes on top of this layer. In this upper layer there are both whole (spherical or quasi-spherical) liposomes, either separate or in small clusters, as well as many that appear to have ruptured, leaving the bilayer debris behind as irregular linear features (Fig. 1 *b*). This rupturing of the liposomes may be due to the cryo-SEM preparation procedure: the sublimation process during this procedure removes the water but does not remove the salt, which may lead to complicated stresses that result in the vesicle rupturing (we note that cryo-SEM pictures of adsorbed HSPC vesicles in pure water (R. Goldberg, A. Schroeder, G. Silbert, K. Torgeman, Y. Barenholz, and J. Klein, unpublished) revealed smooth, unruptured liposomes). The images (e.g., Fig. 1 *b*) reveal that, in contrast to indications from the DLS results obtained in bulk solution, the surface-attached liposomes have a range of sizes: many are ~70 nm in diameter, but others range from 25 to 80 nm or more. This may be attributed to distortions arising from the surface adsorption process (which tends to flatten the liposomes and thus increase their diameter) together with the effect of sequential adsorption on the lateral constraints due to neighboring vesicles (tending to decrease their projection on the

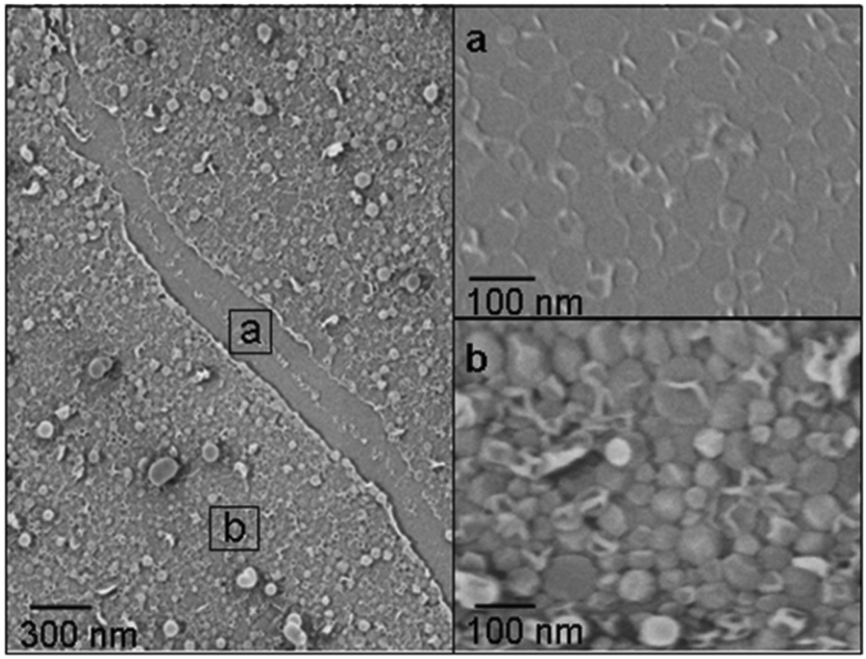

FIGURE 1 Cryo-SEM images of a mica surface coated with HSPC-SUVs in 150 mM $NaNO_3$ salt solution. The left image shows the liposome layers on the mica surface. The feature running diagonally across the image appears to be a tear line in the HSPC layer, which most likely developed during the sample-drying procedure, on either side of which the layers have receded slightly to expose the underlying mica. In such exposed areas, it is possible to view traces of the original quasi-hexagonal close packing of the adsorbed liposome layer on the mica, as shown in the inset in *a* (taken from a different exposed area to that on the left). The inset image in *b* shows the surface topography at a higher magnification, revealing that it is coated with an overlayer of larger and smaller liposome clusters.

surface). An interesting feature can be observed in the region probed by the micrograph in Fig. 1. Presumably due to lateral stresses induced during the cryo-SEM preparation, a mica region that was originally coated with liposomes (region *a*) has been exposed, where on either side the liposome layer has retracted. Traces of the surface-attached liposomes are left behind, revealing (Fig. 1 *a*) a quasi-hexagonal honeycomb pattern arising from the close packing of the liposomes. The cryo-SEM images thus show that the mica surface is covered with a close-packed layer of liposomes, overlaid with an irregular excess of liposomes or small liposome clusters. This implies the presence of surface layers with significant irregular protrusions, which may affect the surface interactions (discussed further below).

SFB: normal force results

Fig. 2 *A* shows normal-force F_n versus surface-separation D profiles between two HSPC-SUV-coated mica surfaces across aqueous 150 mM $NaNO_3$ solution, with the force axis normalized as F_n/R, where R is the radius at the contact region (in the Derjaguin approximation (35)), enabling comparison between different experiments. The inset to Fig. 2 *A*, on a linear-linear scale, reveals attractive forces that cannot be seen in the main log-linear plot. As the surfaces approach from large separations, a clear attraction (*inset* to Fig. 2 *A*) appears at $D = 260 \pm 40$ nm, before the onset of a repulsive regime on further compression. Both the first approach profiles and profiles on subsequent approaches at a given contact point (following shear on the first approach) are shown. The measured forces on approach (*open symbols*) show considerable scatter in both magnitude and range: some approach profiles show no measurable attraction before the repulsive regime, whereas others show a marked attractive well. In contrast, all decompression profiles show a clear attractive well as the surfaces separate. The repulsion upon approach reaches a normalized force value of 2–4 N/m at a "hard wall" separation D_w. The value of D_w was generally 20 ± 2 nm (indicated as *arrow A*), corresponding to the thickness of four stacked bilayers (two fully flattened HSPC-SUVs). In some profiles (at different contact points, indicated as *arrow B*), D_w is in the range of 30 ± 2 nm, corresponding to six stacked bilayers (three flattened HSPC-SUVs) (36).

A simple experiment illustrates the marked attraction seen in the force profiles (Fig. 2 *A*, *inset*). We prepared two identical vials containing 30 mM dispersions of HSPC-SUVs in different solutes. One contained HSPC vesicles both prepared and dispersed in pure water (no added salt), whereas in the other the HSPC vesicles were prepared and dispersed in 150 mM $NaNO_3$. Both vials were held for extended periods at 4°C. The HSPC-SUVs that were held under high salt conditions aggregated and precipitated after ~2 weeks, whereas those in pure water remained dispersed (i.e., with no visible aggregates or sedimentation) for up to many months, as is clearly shown in Fig. 3. Although this demonstration is qualitative (a simple visual inspection showing the absence of turbidity or sedimentation cannot rule out some aggregation of the liposomes), it is consistent with the attraction observed in Fig. 2, as well as with the monotonic repulsion observed previously (R. Goldberg,

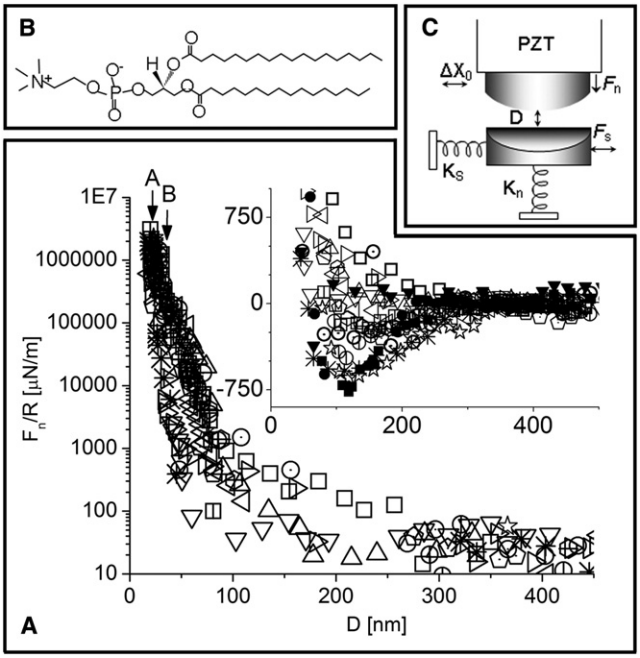

FIGURE 2 (*A*) Profiles of the normal force (F_n/R) versus D, the separation between the surfaces of the two mica sheets coated with the HSPC-SUV layers (where R is the mean mica radius of curvature). Open symbols indicate the approach of the surfaces (decreasing D) and solid symbols indicate separation of the surfaces (increasing D); different symbols correspond to different contact points. Two limiting hard-wall values of D at the highest compressions were observed (for different contact points, as discussed in the text), shown by arrow (*A*: D = 20 ± 2 nm; *B*: D = 30 ± 2 nm). The inset shows the profiles on a linear scale, revealing the existence of a marked attractive-interaction well for some of the approach profiles, and for all of the separation profiles (see text for discussion of this variance). (*B* and *C*) Schematic of the (*B*) HSPC structure and (*C*) SFB (see Klein and Kumacheva (34) and the Supporting Material for a more detailed description of the SFB). The two surfaces are mounted in a crossed-cylindrical configuration whose normal and lateral motion is controlled via the sectored piezoelectric cylinder (PZT), and normal F_n and lateral F_s forces are evaluated from the bending of the two orthogonal springs of constants K_n and K_s, respectively.

A. Schroeder, G. Silbert, K. Torgeman, Y. Barenholz, and J. Klein, unpublished) for interactions between HSPC-SUV layers prepared and measured across pure water.

Shear forces

Shear forces were measured between the mica surfaces coated with the HSPC-SUVs across 150 mM $NaNO_3$ at progressive compressions as the surfaces were made to approach. Lateral (shear) motion with amplitudes Δx_0 in the range of 200–950 nm and velocity v_s (covering a range from ~100 to 2500 nm/s) was applied to the upper mica surface, and the force F_s that was transmitted to the lower mica surface, at different surface separations D, was monitored through the bending of the shear spring (shown schematically in Fig. 2 *C*) (34). Fig. 4 shows typical shear force

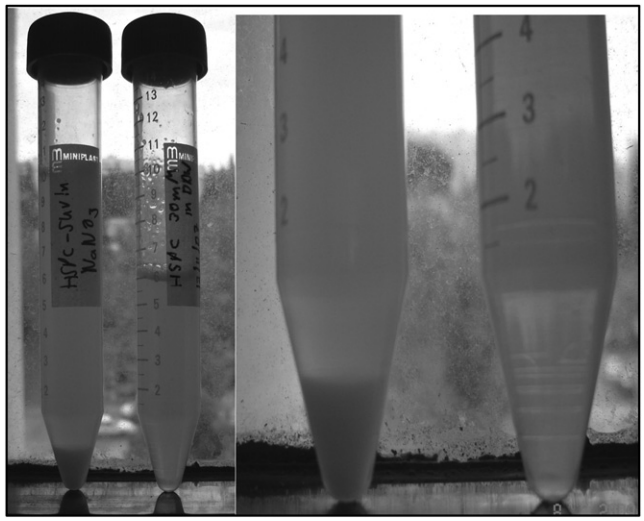

FIGURE 3 The two HSPC 30 mM liposome suspensions in pure water (*right tube*) and 150 mM NaNO3 salt (*left tube*). The two tubes were held at 4°C for extended periods; this image was obtained after 2 months. Whereas the pure water suspension is clear, the salt suspension shows marked sediment (which became visible after only 2 weeks).

measurement outputs, for two different amplitudes and shear velocities at a given contact point. The upper time traces for each set (*d* and *f*) are the applied lateral motion to the upper surface, and the traces below them show the corresponding shear or frictional forces transmitted to the lower surface under different surface separations along with their corresponding pressures. For the set of traces in Fig. 4, there is little measurable transmitted shear force above the noise level for D > ~37 nm, whereas at closer approaches (traces *b*, *c*, and *e*) the shear force as the surfaces slide past each other increases as shown. Trace *a* in Fig. 4 shows for comparison (and as a control) the output when the surfaces are far apart (D ≈ 400 nm) and there is no contact between them. Visual inspection of trace *a* reveals little response, although a frequency analysis (to the right of trace *a*) shows a small response (*arrow*) at the drive frequency (0.5 Hz) arising from coupling due to the thin wires connecting the PZT (34). Such traces were characteristic of all contact points studied, although there was a significant variation between points, as described below. We consider the reasons for this further below.

Fig. 5 shows a graph of F_s versus D determined from traces such as those shown in Fig. 4 from several different contact points and experiments. For D > ~60 ± 20 nm, the magnitude of the measured shear force becomes immeasurably small, even with our high shear force resolution, i.e., it is comparable to the noise level when the surfaces are far apart, as in trace *a* of Fig. 5. However, there is a significant variance, depending on the particular contact point probed, in the separation D_{onset} at which the onset of monotonically increasing F_s with decreasing D begins, from $D_{onset} \approx$ 80 nm to $D_{onset} \approx$ 40 nm. This variance is considered later.

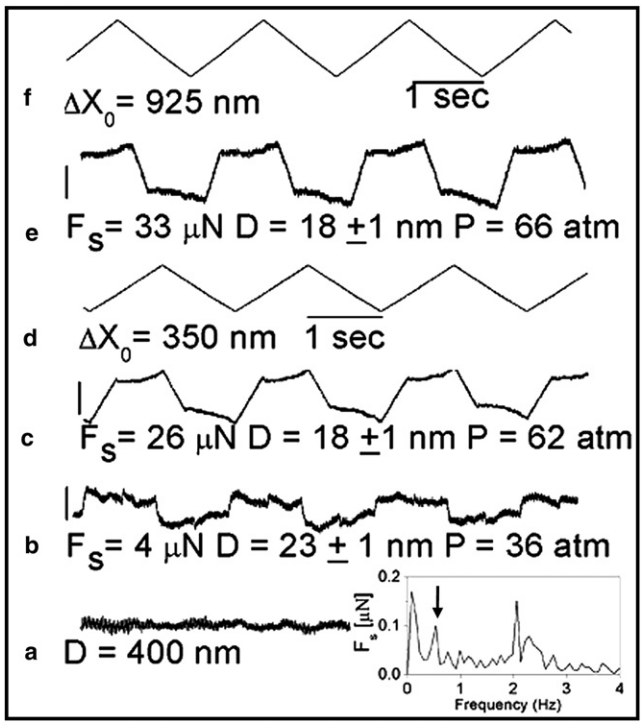

FIGURE 4 Typical shear force F_s versus time traces taken directly from the SFB for a given contact point but at different amplitudes Δx_0 of applied lateral motion and different shear velocities, as well as different compressions (shown both as D-values and as pressures $P = F_n/A$ for the respective traces). Traces were taken for two HSPC-coated surfaces across 150 mM $NaNO_3$. Traces *f* and *d* are the applied shear motion Δx_0, and traces *e* and *a–c* are the respective corresponding traces of the transmitted shear forces. To the right of trace *a*, at large separations where the HSPC layers are not expected to be in contact, the frequency response of the shear forces is shown. At the drive frequency (*arrow*), the response is attributed to coupling via the thin wires connecting to the sectored PZT (34).

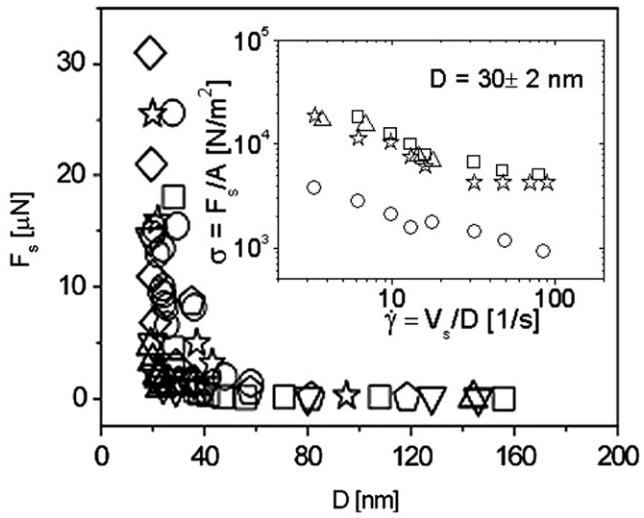

FIGURE 5 Summary of shear force F_s versus surface separation D based on traces as in Fig. 4 (different symbols refer to different contact points). (*Inset*) The variation of the shear stress σ, defined as $\sigma = F_s/A$, where A is the Hertzian contact area, as a function of the shear rate $\dot{\gamma}$, where $\dot{\gamma} = v_s/D$, v_s is the shear velocity and D is the separation between the two opposing surfaces; symbols correspond to contact points in the main figure.

The inset to Fig. 5 shows the effect of shear velocity v_s on the shear force F_s for a given surface separation D (in a high compression regime). The data are plotted as shear stress $\sigma = F_s/A$ versus shear rate $\dot{\gamma} = v_s/D$, where A is the flattened area of contact between the surfaces. The A value can be evaluated from the Hertzian contact mechanics relation (37): $A = \pi(F_nR/K)^{2/3}$, where $K = (5 \pm 1) \times 10^9$ N/m^2 is an effective modulus of the glue/mica substrate combination derived by separately measuring A as a function of load F_n (not shown). The major effect seen in the σ versus $\dot{\gamma}$ variation is that the shear rate dependence of the frictional force is weak, with only a threefold reduction in F_s over a nearly two orders of magnitude increase in $\dot{\gamma}$; this weak shear rate dependence applies to all experiments and contact positions measured. We also see a considerable variance in the magnitude of F_s between different contact points at similar D-values (lower and upper sets of data points), a point we will return to later.

Fig. 6 shows a plot of the shear force F_s as a function of the applied normal force F_n. The magnitude of the effective friction coefficient $\mu = \partial F_s/\partial F_n$ is seen to be in the range $\mu \approx 6 \times 10^{-4}$ to 8×10^{-3} at pressures up to ~6 MPa (~60 atmospheres), a significant variation that we will discuss later. Although this value is low to very low, it is still significantly higher than the extremely low values found for friction coefficients between layers of HSPC liposomes in pure water (μ-values in pure water were in the range of 2×10^{-5} to 10^{-4}) (R. Goldberg, A. Schroeder, G. Silbert, K. Torgeman, Y. Barenholz, and J. Klein, unpublished).

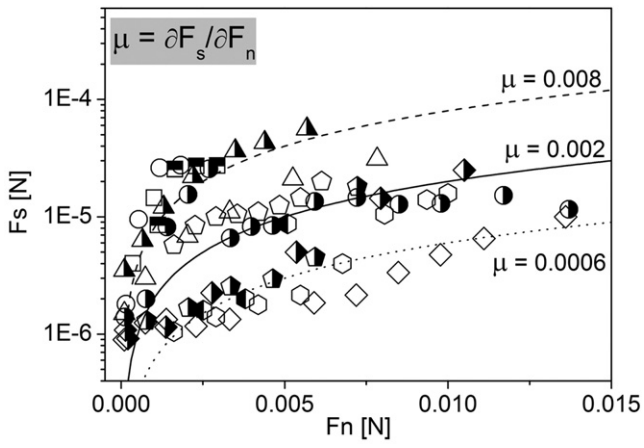

FIGURE 6 Shear force F_s as a function of the normal force F_n compressing the surfaces. Open symbols: first entry to contact point; half-solid symbols: second entry (different symbols refer to different contact points). The friction coefficient, defined as $\mu = \partial F_s/\partial F_n$, is shown as the curves for three different values of μ.

DISCUSSION

The main findings of this study concern the normal and lateral interactions that occur between two molecularly smooth substrates coated with a layer of HSPC-SUVs that adsorb spontaneously from a dispersion of the vesicles. In contrast to our earlier study (R. Goldberg, A. Schroeder, G. Silbert, K. Torgeman, Y. Barenholz, and J. Klein, unpublished) of such interactions across pure water (no added salt), in the work presented here, the liposome dispersion and the medium across which the interactions were measured were at high salt concentration (150 mM $NaNO_3$). This was done to better emulate interactions between layers of PC lipids (which constitute the liposome membranes), in particular the shear and frictional interactions between them, at physiological salt levels. Such PC layers have been conjectured, with some controversy (26), to be of central importance for biological lubrication processes, particularly at synovial joints (31,38–40).

The attachment of liposomes from their dispersion onto the mica surfaces to form close-packed layers covered by additional vesicles (as revealed in the cryo-SEM micrographs) is driven by two factors. The adherence to the negatively charged mica surface arises from the attraction of the phosphocholine headgroup dipoles (structure in Fig. 2 *B*) exposed at the liposome membrane (41) (we emphasize here the overall neutrality of the zwitterionic HSPC as revealed by the ζ-potential measurements). This was shown explicitly in our previous study of the same liposomes in pure water (R. Goldberg, A. Schroeder, G. Silbert, K. Torgeman, Y. Barenholz, and J. Klein, unpublished), in which an attraction was directly measured between a layer of the HSPC vesicles and a bare mica surface. On top of the close-packed, surface-attached HSPC-SUV layer, we see an overlayer of additional vesicles, either individually or in small clusters. We attribute the attachment of these additional vesicles in the overlayer on top of each close-packed liposome monolayer to the attraction in these high-salt conditions between the liposomes seen in the normal force profiles (Fig. 2 *A, inset*) discussed below. The irregularity of this overlayer is attributed to the effect of the washing conditions, which may have removed some (but clearly not all) of the adsorbed vesicles within the overlayer.

A clear attraction is seen in some of the approach profiles (*open symbols*, Fig. 2 *A, inset*), setting on from ~300 nm and becoming repulsive on further approach at $D <$ ~50–80 nm. Other approach profiles apparently do not show a clear attractive well before repulsion occurs. Upon separation after strong compression (*solid symbols*), all profiles show an attractive well, which disappears (within the scatter) at $D >$ ~300 nm. We note that in our earlier study in pure water (no added salt) (R. Goldberg, A. Schroeder, G. Silbert, K. Torgeman, Y. Barenholz, and J. Klein, unpublished), the normal interactions were always monotonically repulsive, upon both approach and separation. Therefore, the marked attraction observed in this study arises from the added salt. The added salt can influence the liposome-liposome interactions in two ways: First, it greatly reduces the Debye screening length relative to pure water. This serves to eliminate the long-ranged repulsion between the surfaces that was attributed in our previous study (R. Goldberg, A. Schroeder, G. Silbert, K. Torgeman, Y. Barenholz, and J. Klein, unpublished) to residual charges either on the mica or on the liposome layers themselves (here, our measurements (see Materials and Methods) hint at a small ζ potential at low salt concentration (42,43)). Second, the inorganic ions (mainly Na^+) compete with the lipid molecules for water of hydration (44), and as a result the extent of hydration of the phosphocholine headgroups is reduced, an effect that has been measured directly (45). This will be referred to later in the context of its effect on the hydration lubrication mechanism, but it will also reduce the hydration repulsion between the liposomes, enhancing any net attraction. The attraction itself may be attributed to van der Waals interactions and/or attractive dipole-dipole interactions that may arise from correlated positioning of the opposing zwitterionic headgroups. Both are previously suggested mechanisms of attraction between PC layers (12,13). The strong repulsion regime at high compressions is attributed to steric compression of the liposome layers, with possibly a squeezing-out of liposomes in the overlayer at the highest compressions. As noted in Fig. 2 *A*, there were indications of a bimodal distribution of the hard wall at the highest compressions in this study, depending on the contact point: either 20 ± 2 nm (most of the profiles; *arrow A* in Fig. 2 *A*) or 30 ± 2 nm (some profiles; *arrow B*). We attribute these values to two flattened liposome layers or three flattened liposome layers, respectively, where in the latter case the two-surfaces-attached layers trap an additional liposome layer between them.

This picture, therefore, is one in which the surface-adsorbed liposomes do not rupture but retain their closed structure even at the highest compressions (up to ~60 atm) attained in this study. We believe this robustness results from the HSPC vesicles being in the rigid gel phase, and their close packing on the surface. We note that when 1-palmitoyl-2-oleoyl-*sn*-glycero-3-phosphocholine (POPC) liposomes, which are in the much less rigid liquid-crystalline phase, are used (R. Goldberg, A. Schroeder, G. Silbert, K. Torgeman, Y. Barenholz, and J. Klein, unpublished), the data indicate that, unlike the more-rigid HSPC vesicles, they undergo rupture and consequent squeeze-out from between the surfaces.

It is instructive to consider the origin of the significant variance seen in the normal force profiles. This is particularly striking in the inset to Fig. 2 *A*: some of the profiles show a clear attractive well on approach, whereas others appear to show a monotonic repulsion. We attribute the origin of this behavior to the irregular topology of the interacting liposome layers. This is illustrated schematically in

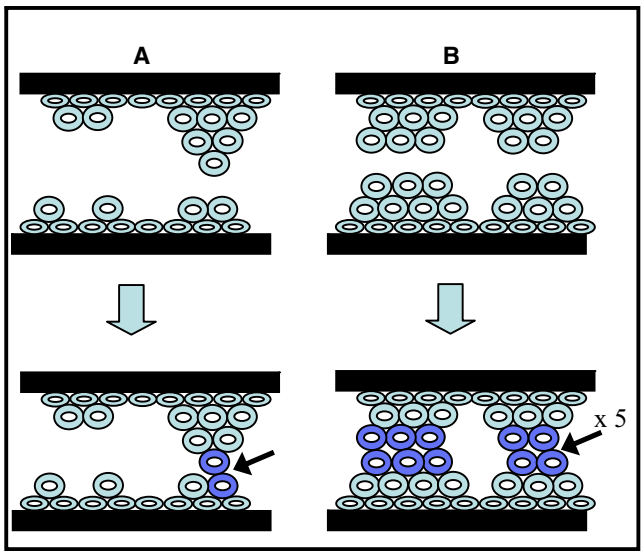

FIGURE 7 Schematic illustration based on topography observed in cryo-SEM micrograph images (e.g., as in Fig. 1) of possible modes of initial overlap between different clustering patterns of the liposomes (note that surface-attached liposomes are shown as more compressed, due to attractions to the surface, than the liposomes in the overlayer). In panel *A* the large cluster makes initial (attractive) contact at one point (*darker-shaded liposomes*); for approach to further attractive contacts, a large repulsion associated with compressive distortion of the liposome cluster must be overcome. In panel *B*, the initial contact occurs between several pairs of liposomes at once, resulting in a larger initial attraction. See text for a more detailed discussion.

Fig. 7. From the cryo-SEM pictures (Fig. 1) we can see that the overlayer of liposomes on the close-packed, surface-attached liposome layer contains both larger and smaller clusters of liposomes. When a larger cluster dominates the interacting region, as indicated in Fig. 7 *A*, there is a smaller initial contact area when the liposomes in the overlayers of the opposing surfaces first come into overlap. This results in less attraction as fewer of the liposomes interact, as shown by the darker-shaded liposomes in Fig. 7 *A*. To access more of the attractive liposome-liposome interactions, the larger cluster must be compressed, and this results in a repulsive force of steric origin. Because these repulsions (due to compressively distorting the liposomes) are much larger than the weak attractive interaction between the few contacts, the repulsion will dominate the initial interactions, and the overall effective force versus distance profile for such contact regions will be repulsive. If, on the other hand, a particular contact point is associated with interacting regions that are smoother and have no large protruding clusters, as indicated schematically in Fig. 7 *B*, the initial interaction between them will involve the simultaneous attractive contact of several liposomes, as indicated by the darker-shaded vesicles in Fig. 7 *B* (*bottom*). Because each such contact is associated with an attractive force, there will be a larger overall initial attraction for such flatter contact positions (hence the net attractive well) before the steric compression results in the repulsive wall. This simple qualitative explanation has an explicit consequence for the shear/frictional forces, which we examine below.

The shear force profiles (Fig. 4), as summarized in Fig. 5 and especially in the friction versus load plot of Fig. 6, reveal a number of important features. The most striking one is the low (0.008) to very low (0.0006) friction coefficient seen in Fig. 6 up to local contact pressures (F_n/A) of ~60 atm (~6 MPa). We attribute this low friction as the liposome layers slide past each other to the hydration lubrication mechanism, which has emerged as a new paradigm for the reduction of friction in aqueous environments. This was first described in the context of hydrated ions trapped between sliding charged surfaces (46), and has also been observed, though at much lower pressures than used in this study, only up to ~0.3 MPa, for physisorbed polyelectrolyte brushes (23), surfactants under water (47), and supported lipid bilayers (24). In a more recent study, highly hydrated polyzwitterion brushes (25) covalently grafted from solid substrates proved to be capable of reducing friction coefficients to low levels similar to those observed here at pressures up to 7 MPa. In particular, our previous study (R. Goldberg, A. Schroeder, G. Silbert, K. Torgeman, Y. Barenholz, and J. Klein, unpublished) on the same HSPC-SUV liposomes, coating mica surfaces in pure water, showed remarkably low friction coefficients down to $\mu = \sim 10^{-5}$ at pressures of up to 12 MPa. In both of these recent high-pressure studies, the low friction was also attributed to the hydration lubrication mechanism. According to this concept (46), the low friction is due to hydration layers that are tenaciously attached and therefore resistant to being squeezed out under high pressures, while at the same time they have rapid relaxation times (typically on the order of nanoseconds for hydration layers surrounding the alkali metal ions) and thus respond in a very fluid manner under shear. This combination means that layers of hydrated species can support a large normal stress while sliding easily past each other, which is the molecular origin of the very efficient hydration lubrication. In the case of the HSPC liposome layers used here, this is provided by the outer surfaces of the vesicles (fully covering the underlying substrates) exposing the highly hydrated phosphocholine groups, which (depending on the means of measurement) have been reported to contain up to 15 water molecules in the primary hydration shell (15,48–50).

It is appropriate at this point to remark on the large variance in the friction coefficient (Fig. 6). We believe that this is due to the different topology associated with liposome clusters in the overlayer at different contact points (illustrated in Fig. 7), to which we also attributed the variance in the normal forces. Thus, for the case of large clusters making initial contact when the opposing surfaces come into overlap, as in Fig. 7 *A*, we would expect the sliding to result in considerable plowing and distortion of these contacting clusters. The frictional dissipation would then be

significantly larger than for the case of the opposing surfaces being smoother, and making initial simultaneous contact at large numbers of points, as schematically shown in Fig. 7 *B*. In that case, there would be less plowing dissipation, and the frictional forces would be largely due to sliding of the exposed hydrated phosphocholine groups past each other, where the hydration lubrication mechanism is active. If this explanation is indeed correct, we would expect those contact points corresponding to Fig. 7 *A* to have a larger friction (due to the plowing dissipation of the larger clusters) and at the same to show less attraction on approach, as discussed above. A careful examination of the data for different points shows that this is in fact the case. For all contact points measured, both within the same experiment and across different experiments, the higher friction coefficients in Fig. 6 correspond to $F_n(D)$ profiles in Fig. 2, inset, that exhibit monotonic repulsion, whereas the lower friction coefficients in Fig. 6 correspond to approach profiles that show a clear attractive well. This surprising correlation of lower friction with larger adhesion is somewhat counterintuitive, as one would expect a larger adhesive interaction to correspond to a larger frictional force, and a larger repulsion to be associated with a lower friction, whereas in fact the opposite is the case. However, this picture fits well with our attribution of the variance in both normal and frictional forces to the local topography of liposome clusters at the different contact points.

A corollary to the above conclusions is that the intrinsic frictional forces between the liposome layers sliding past each other corresponds to the lower level of friction coefficients measured, i.e., to $\mu = \sim\leq 0.0006$ at pressures up to 6 MPa. The higher friction coefficients measured (up to $\mu = \sim 0.008$ in Fig. 6) are a result in part of the rougher surface topology at the contact points at which they were measured, and to the consequent plowing dissipation noted above. These values (i.e., $\mu = \sim\leq 0.0006$ at pressures up to 6 MPa) are much lower than reported in some of the previous studies of hydration lubrication at lower pressures in aqueous systems, including those noted earlier (23,24), though they are somewhat higher than observed for HSPC-SUV lubricants in pure water (R. Goldberg, A. Schroeder, G. Silbert, K. Torgeman, Y. Barenholz, and J. Klein, unpublished). The higher friction coefficients of the liposome layers at physiological-level salt concentrations relative to pure water are probably due to competition of the inorganic ions (Na^+ in this study) for the water of hydration (51), which reduces the efficiency of the hydration lubrication mechanism. Similar reductions in lubrication efficiency with increasing salt concentrations were also observed in a study by Chen et al. (25) on highly hydrated poly(zwitterionic) brushes, and likewise attributed. Nonetheless, even at the higher level of friction at the high salt condition used here, the magnitude of the friction coefficient, $\mu = 0.0006$ (0.15 M $NaNO_3$) up to at least 60 atm pressure, compares well with values of cartilage-cartilage friction at similarly high pressures and salt concentrations in the major human joints (26,28).

In conclusion, we studied the lubrication afforded by liposome layers attached to solid surfaces when two such surfaces are compressed and made to slide past each other, at pressures up to ~60 atm and salt concentrations of 0.15 M $NaNO_3$. These salt and pressure conditions are similar to those found in the physiological environments of major joints (e.g., human hips and knees), and the friction coefficients measured ($\mu = \sim 0.0006$) are comparable to or lower than those observed in healthy joints. The origin of this low friction is the hydration lubrication mechanism that is active between the phosphocholine groups exposed by the liposomes. Apart from their practical potential for technological and biomedical applications, these findings provide support for the conjecture that lubrication in the major joints may be mediated, at least in part, by PC lipid layers, where the sliding interfaces consist of hydrated phosphocholine groups that are essentially identical to those exposed by the HSPC vesicles.

SUPPORTING MATERIAL

Additional text and references are available at http://www.biophysj.org/biophysj/supplemental/S0006-3495(11)00419-X.

We thank Dr. Eyal Shimoni (Electron Microscope Unit, Weizmann Institute, Rehovot, Israel) for his help with the cryo-SEM imaging.

This study was supported by the Israel Science Foundation, European Research Council, Charles W. McCutchen Foundation, Minerva Foundation (Weizmann Institute), and Barenholz Fund (Hebrew University).

REFERENCES

1. Barenholz, Y., and S. Amselem. 1993. Liposome Technology. CRC Press, Boca Raton, FL.
2. Lasic, D. D., and D. Needham. 1995. The 'stealth' liposome: a prototypical biomaterial. *Chem. Rev.* 95:2601–2608.
3. Banerjee, R. 2001. Liposomes: applications in medicine. *J. Biomater. Appl.* 16:3–21.
4. Pohorille, A., and D. Deamer. 2002. Artificial cells: prospects for biotechnology. *Trends Biotechnol.* 20:123–128.
5. Bangham, A. D. 1972. Lipid bilayers and biomembranes. *Annu. Rev. Biochem.* 41:753–776.
6. Bordi, F., C. Cametti, …, S. Sennato. 2005. Large equilibrium clusters in low-density aqueous suspensions of polyelectrolyte-liposome complexes: a phenomenological model. *Phys. Rev. E Stat. Nonlin. Soft Matter Phys.* 71:050401.
7. Bordi, F., C. Cametti, …, D. Truzzolillo. 2007. Strong repulsive interactions in polyelectrolyte-liposome clusters close to the isoelectric point: a sign of an arrested state. *Phys. Rev. E Stat. Nonlin. Soft Matter Phys.* 76:061403.
8. Maza, A. D., A. M. Manich, and J. L. Parra. 1997. Intermediate aggregates resulting in the interaction of bile salt with liposomes studied by transmission electron microscopy and light scattering techniques. *J. Microsc.* 186:75–83.
9. Liu, D. Z., W. Y. Chen, …, S. P. Yang. 2000. Microcalorimetric and shear studies on the effects of cholesterol on the physical stability of lipid vesicles. *Colloids Surf. A.* 172:57–67.

10. Sabín, J., G. Prieto, …, F. Sarmiento. 2007. Fractal aggregates induced by liposome-liposome interaction in the presence of Ca^{2+}. *Eur. Phys. J. E Soft Matter.* 24:201–210.

11. Garbuzenko, O., Y. Barenholz, and A. Priev. 2005. Effect of grafted PEG on liposome size and on compressibility and packing of lipid bilayer. *Chem. Phys. Lipids.* 135:117–129.

12. Rand, R. P., N. L. Fuller, …, D. C. Rau. 1988. Variation in hydration forces between neutral phospholipid bilayers: evidence for hydration attraction. *Biochemistry.* 27:7711–7722.

13. Marra, J., and J. Israelachvili. 1985. Direct measurements of forces between phosphatidylcholine and phosphatidylethanolamine bilayers in aqueous electrolyte solutions. *Biochemistry.* 24:4608–4618.

14. Parsegian, V. A., and P. R. Rand. 1995. Interaction in membrane assemblies. *In* Handbook of Biological Physics. R. Lipowsky and E. Sackman, editors. Elsevier Science B.V., Amsterdam. 643–690.

15. Rand, R. P., and V. A. Parsegian. 1989. Hydration forces between phospholipid bilayers. *Biochim. Biophys. Acta.* 988:351–376.

16. Leikin, S., V. A. Parsegian, …, R. P. Rand. 1993. Hydration forces. *Annu. Rev. Phys. Chem.* 44:369–395.

17. Schneider, J., Y. F. Dufrêne, …, G. U. Lee. 2000. Atomic force microscope image contrast mechanisms on supported lipid bilayers. *Biophys. J.* 79:1107–1118.

18. Liang, X., G. Mao, and K. Y. Simon Ng. 2004. Probing small unilamellar EggPC vesicles on mica surface by atomic force microscopy. *Colloids Surf. B Biointerfaces.* 34:41–51.

19. Egawa, H., and K. Furusawa. 1999. Liposome adhesion on mica surface studied by atomic force microscopy. *Langmuir.* 15:1660–1666.

20. Jass, J., T. Tjärnhage, and G. Puu. 2000. From liposomes to supported, planar bilayer structures on hydrophilic and hydrophobic surfaces: an atomic force microscopy study. *Biophys. J.* 79:3153–3163.

21. Schönherr, H., J. M. Johnson, …, S. G. Boxer. 2004. Vesicle adsorption and lipid bilayer formation on glass studied by atomic force microscopy. *Langmuir.* 20:11600–11606.

22. Reference deleted in proof.

23. Raviv, U., S. Giasson, …, J. Klein. 2003. Lubrication by charged polymers. *Nature.* 425:163–165.

24. Trunfio-Sfarghiu, A. M., Y. Berthier, …, J. P. Rieu. 2008. Role of nanomechanical properties in the tribological performance of phospholipid biomimetic surfaces. *Langmuir.* 24:8765–8771.

25. Chen, M., W. H. Briscoe, …, J. Klein. 2009. Lubrication at physiological pressures by polyzwitterionic brushes. *Science.* 323:1698–1701.

26. Hills, B. A., and G. D. Jay. 2002. Identity of the joint lubricant. *J. Rheumatol.* 29:200–201.

27. Sivan, S., A. Schroeder, …, Y. Barenholz. 2010. Liposomes act as effective biolubricants for friction reduction in human synovial joints. *Langmuir.* 26:1107–1116.

28. Swann, D. A., K. J. Bloch, …, E. Shore. 1984. The lubricating activity of human synovial fluids. *Arthritis Rheum.* 27:552–556.

29. Maroudas, A. 1967. Hyaluronic acid films. Lubrication and wear in living and artificial human joints. *Proc. Inst. Mech. Eng.* 181:122–124.

30. Han, L., D. M. Dean, …, A. J. Grodzinsky. 2007. Lateral nanomechanics of cartilage aggrecan macromolecules. *Biophys. J.* 92:1384–1398.

31. Hills, B. A., and B. D. Butler. 1984. Surfactants identified in synovial fluid and their ability to act as boundary lubricants. *Ann. Rheum. Dis.* 43:641–648.

32. Lichtenberg, D., and Y. Barenholz. 1988. Liposomes: preparation, characterization, and preservation. *Methods Biochem. Anal.* 33: 337–462.

33. Shmeeda, H., S. Even-Chen, …, Y. Barenholz. 2003. Enzymatic assays for quality control and pharmacokinetics of liposome formulations: comparison with nonenzymatic conventional methodologies. *Methods Enzymol.* 367:272–292.

34. Klein, J., and E. Kumacheva. 1998. Simple liquid confined to molecularly thin layers. I. Confinement-induced liquid-to-solid phase transitions. *J. Chem. Phys.* 108:6996–7009.

35. Derjaguin, B. V., N. V. Churaev, and V. M. Muller. 1987. Surface Forces. Plenum, New York.

36. Janshoff, A., and C. Steinem. 2001. Scanning force microscopy of artificial membranes. *ChemBioChem.* 2:798–808.

37. Johnson, K. L. 2004. Contact Mechanics. Cambridge University Press, London.

38. Hills, B. A., and M. K. Monds. 1998. Deficiency of lubricating surfactant lining the articular surfaces of replaced hips and knees. *Br. J. Rheumatol.* 37:143–147.

39. Pawlak, Z., and A. Oloyede. 2008. Conceptualisation of articular cartilage as a giant reverse micelle: a hypothetical mechanism for joint biocushioning and lubrication. *Biosystems.* 94:193–201.

40. Potvin, J. R., R. W. Norman, and S. M. McGill. 1991. Reduction in anterior shear forces on the L4/L5 disc by the lumbar musculature. *Clin. Biomech. (Bristol, Avon).* 6:88–96.

41. Pauling, L. 1930. The structure of the micas and related minerals. *Proc. Natl. Acad. Sci. USA.* 16:123–129.

42. Jones, M. N. 1995. The surface properties of phospholipid liposome systems and their characterisation. *Adv. Colloid Interface Sci.* 54: 93–128.

43. Oku, N., and R. C. MacDonald. 1983. Differential effects of alkali metal chlorides on formation of giant liposomes by freezing and thawing and dialysis. *Biochemistry.* 22:855–863.

44. Hauser, H. 1991. Effect of inorganic cations on phase transitions. *Chem. Phys. Lipids.* 57:309–325.

45. Rappolt, M., G. Pabst, …, P. Laggner. 2001. Salt-induced phase separation in the liquid crystalline phase of phosphatidylcholines. *Colloids Surf. A Physicochem. Eng. Asp.* 183:171–181.

46. Raviv, U., and J. Klein. 2002. Fluidity of bound hydration layers. *Science.* 297:1540–1543.

47. Briscoe, W. H., S. Titmuss, …, J. Klein. 2006. Boundary lubrication under water. *Nature.* 444:191–194.

48. Nagle, J. F., R. Zhang, …, R. M. Suter. 1996. X-ray structure determination of fully hydrated L alpha phase dipalmitoylphosphatidylcholine bilayers. *Biophys. J.* 70:1419–1431.

49. Pabst, G., M. Rappolt, …, P. Laggner. 2000. Structural information from multilamellar liposomes at full hydration: full q-range fitting with high quality x-ray data. *Phys. Rev. E Stat. Phys. Plasmas Fluids Relat. Interdiscip. Topics.* 62(3 Pt B):4000–4009.

50. Yaseen, M., J. R. Lu, …, J. Penfold. 2006. The structure of zwitterionic phosphocholine surfactant monolayers. *Langmuir.* 22:5825–5832.

51. Clarke, R. J., and C. Lüpfert. 1999. Influence of anions and cations on the dipole potential of phosphatidylcholine vesicles: a basis for the Hofmeister effect. *Biophys. J.* 76:2614–2624.